Article

Alanine-Scanning Mutagenesis of α-Conotoxin GI Reveals the Residues Crucial for Activity at the Muscle Acetylcholine Receptor

Jiong Ning, Rui Li, Jie Ren, Dongting Zhangsun, Xiaopeng Zhu, Yong Wu * and Sulan Luo *

Key Laboratory of Tropical Biological Resources, Ministry of Education, Key Lab for Marine Drugs of Haikou, Hainan University, Haikou 570228, Hainan, China; ningjiong2018@163.com (J.N.); flychcken@163.com (R.L.); hndx2303@163.com (J.R.); zhangsundt@163.com (D.Z.); zhuxiaopeng@hainu.edu.cn (X.Z.)
* Correspondence: wuyong@hainu.edu.cn (Y.W.); luosulan2003@163.com (S.L.)

check for updates

Abstract: Recently, the muscle-type nicotinic acetylcholine receptors (nAChRs) have been pursued as a potential target of several diseases, including myogenic disorders, muscle dystrophies and myasthenia gravis, etc. α-conotoxin GI isolated from *Conus geographus* selectively and potently inhibited the muscle-type nAChRs which can be developed as a tool to study them. Herein, alanine scanning mutagenesis was used to reveal the structure–activity relationship (SAR) between GI and mouse $\alpha1\beta1\delta\varepsilon$ nAChRs. The Pro^5, Gly^8, Arg^9, and Tyr^{11} were proved to be the critical residues for receptor inhibiting as the alanine (Ala) replacement led to a significant potency loss on mouse $\alpha1\beta1\delta\varepsilon$ nAChR. On the contrary, substituting Asn^4, His^{10} and Ser^{12} with Ala respectively did not affect its activity. Interestingly, the [E1A] GI analogue exhibited a three-fold potency for mouse $\alpha1\beta1\delta\varepsilon$ nAChR, whereas it obviously decreased potency at rat $\alpha9\alpha10$ nAChR compared to wildtype GI. Molecular dynamic simulations also suggest that loop2 of GI significantly affects the interaction with $\alpha1\beta1\delta\varepsilon$ nAChR, and Tyr^{11} of GI is a critical residue binding with three hydrophobic amino acids of the δ subunit, including Leu^{93}, Tyr^{95} and Leu^{103}. Our research elucidates the interaction of GI and mouse $\alpha1\beta1\delta\varepsilon$ nAChR in detail that will help to develop the novel analogues of GI.

Keywords: muscle-type nAChRs; α-conotoxin GI; structure-activity relationship; electrophysiological study; molecular dynamic simulations

1. Introduction

Nicotinic acetylcholine receptors (nAChRs) are a member of ligand-gated ion channels that mediate the fast excitatory cholinergic neurotransmission in the central and peripheral nervous system [1–3]. In vertebrates, nAChRs are classified into muscle-type and neuronal-type nAChRs based on their primary sites of expression. The muscle-type nAChRs are found at the neuromuscular junction, and they mediate neuromuscular transmission at the neuromuscular junction (NMJ) [4,5]. Noticeably, muscle-type receptors from fetal muscle are composed of a combination of $\alpha1\beta1\delta\gamma$ subunits whereas those from adult muscle have the composition of $\alpha1\beta1\delta\varepsilon$ subunit. Previous research revealed that the muscle-type nAChRs were implicated in pathophysiology conditions, including myasthenia gravis, rhabdomyosarcoma, muscle dystrophies, and muscle atrophy [6–8].

Conus is a genus of marine gastropod molluscs which is estimated to have 700 different species distributing in tropical and sub-tropical oceans [9,10]. These gastropods armed with deadly venoms can capture worms, fishes or other mollusks. The venoms are composed of different kinds of bioactive peptides which are named as conotoxins [11,12]. Based on their conserved signal peptide sequences, the various conotoxins are classified into different super families. Further classification into

families depends on their patterns of disulfide and pharmacological activities [10,13,14]. Among the conotoxins, α-conotoxins are the most studied and targeted muscle-type or neuronal-type nAChRs with high affinity and selectivity. Typical α-conotoxins are arranged in a CC-Xm-C-Yn-C pattern with two loops and have four cysteine residues to form two disulfide bonds with CysI-CysIII and CysI-CysIV connectivity. The first loop (X_m) contains three or four amino acids (m = 3–4) and the second loop (Y_n) consists of three to seven amino acids (n = 3–7) [15,16]. Interestingly, most α-3/5 family conotoxins block muscle-type nAChRs with high potency.

α-conotoxin GI, which was isolated from the *Conus geographus* venom, is composed of 13 amino acids that selectively inhibited muscle-type nAChRs with the IC_{50} of 20 nM [17,18]. The structure of GI was firstly determined by two-dimensional NMR [19]. Meanwhile, several studies revealed the binding molecular mechanism between GI and muscle-type nAChRs [20,21]. Hann et al. found the 9-arginine of GI was critical for its high selectivity and activity [22], and Geobe et al. also demonstrated that α-conotoxin [R9A] GI displayed a decrease in affinity for the two acetylcholine-binding sites on *Torpedo* receptors [23]. However, the role of each amino acid in α-conotoxin GI has remained unidentified [19,24,25]. Nowadays, alanine scanning mutagenesis has become an effective strategy in exploring the relationship between toxins and receptors and has been applied in the α-conotoxins pivotal residue identification [26,27].

In the present study, a series of GI analogues were synthesized and the inhibitory activity on various nAChR subunits were assessed (Figure 1). The results demonstrated that the activities retained for [N4A] GI, [H10A] GI and [S12A] GI compared to GI, whereas their potency decreased nearly more than 10-fold for [P5A] GI, [G8A] GI, [R9A] GI, and [Y11A] GI. More importantly, replacing Glu[1] with an Ala led to a three-fold increase in potency at the α1β1δε subtype. Further investigation revealed the interaction between α-conotoxin GI and muscle-type nAChRs. In addition, these analogues have the potential to be developed as a molecular probe for differentiating the subtype of nAChRs [28,29].


Figure 1. Sequences of α-conotoxin GI and its analogues. Each substituted alanine is labeled in bold and blue. The connectivity of Cysteine (CysI-CysIII, CysII-CysIV) is marked in bold and red. * indicates a C-terminal amide.

2. Results

2.1. Synthesis and Purification of GI and Its Analogues

In this study, standard Fmoc solid phase peptide synthesis strategy was used to synthesize GI and its mutants. A two-step oxidation protocol was used to fold these peptides as described previously [30]. Briefly, CysI and CysIII were protected with S-trityl (S-Trt) while CysII and CysIV were protected with S-acetamidomethyl (S-Acm). The first disulfide bridge between CysI and CysIII was formed using the potassium ferricyanide oxidation method, and then the second disulfide bond was produced

through iodine oxidation. All synthesized peptides were monitored by analytical Reversed-Phase High Performance Liquid Chromatography (RP-HPLC), and the purity of each analogue was above 95%. Typically, the retention of the fully oxidized peptide GI and [E1A] GI is 8.82 and 8.57 min respectively, and the molecular weight of GI and [E1A] GI is 1436.50 and 1378.52 Da respectively, which are identical with the theoretical molecular weight (Figure 2). The HPLC chromatogram and ESI-MS (Electrospray ionization mass spectrometry) data of other GI analogues are provided in the Supplementary Materials' Figures S1–S3.
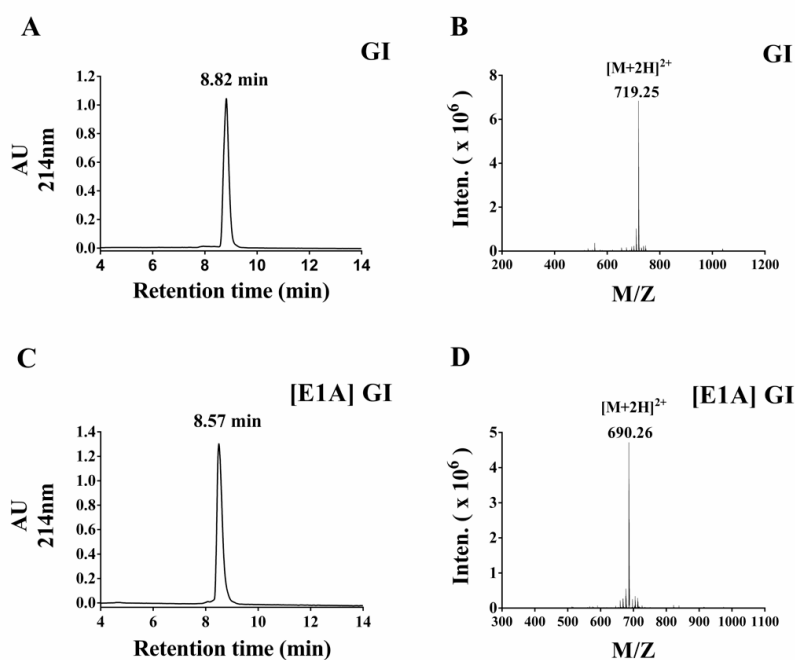

Figure 2. The HPLC and ESI-MS profiles of α-conotoxin GI and α-conotoxin [E1A] GI. The peptide GI and [E1A] GI were analyzed on a reverse-phase analytical Vydac C18 column with a solvent gradient from 5% buffer B to 40% buffer B for 20 min where buffer A = 0.075% trifluoroacetic acid (TFA), remainder H_2O and buffer B = 0.050% TFA, 90% acetonitrile, remainder H_2O. The absorbance was monitored at 214 nm. (**A**) The HPLC chromatogram of fully oxidized peptide GI; (**B**) ESI-MS data for GI with an observed monoisotopic mass of 1436.50 Da; (**C**) the HPLC chromatogram of fully folded peptide [E1A] GI; (**D**) ESI-MS data for [E1A] GI with an observed monoisotopic mass of 1378.52 Da.

2.2. Potency of α-Conotoxin GI and Its Analogues at the Mouse $\alpha1\beta1\delta\varepsilon$ nAChR

To better understand the SAR between GI and muscle-type nAChRs, GI and all analogues were firstly tested on mouse $\alpha1\beta1\delta\varepsilon$ nAChR at a single concentration of 10 nM. Figure 3 indicates that the relative amount of inhibitions are evoked by all peptides. Three analogues replacing Asn[4], His[10] and Ser[12] with Ala had little effect on $\alpha1\beta1\delta\varepsilon$ nAChR compared with native GI (67% inhibition). On the contrary, [P5A] GI and [R9A] GI substantially reduced the activity, they exhibited 21.9% and 17.6% inhibition of relative current amplitude. In addition, [G8A] GI and [Y11A] GI analogues resulted in a complete loss of inhibitory activity at the concentration of 10 nM. Notably, only one alanine substitution [E1A] GI showed a significant increase at mouse $\alpha1\beta1\delta\varepsilon$ nAChR *versus* GI, completely blocking muscle-type nAChR at the concentration of 10 nM.

We also observed that the alanine-substituted analogues affected not only the potency against $\alpha1\beta1\delta\varepsilon$ nAChR but also its current recovery. Meanwhile, Figure 4 illustrates the effects of [Y11A] GI and [E1A] GI on mouse $\alpha1\beta1\delta\varepsilon$ nAChR-mediated current respectively. We could see that GI blockade of mouse $\alpha1\beta1\delta\varepsilon$ nAChR was 75.5% at the concentration of 10 nM, while full blocking of ACh-evoked currents was obtained with 10 nM [E1A] GI. Additionally, the recovery time (50% initial current) was compared between wild peptide GI and mutant [E1A] GI after the blockade by 10 nM toxin.

Complete recovery of [E1A] GI was observed within 4 min after α-conotoxin [E1A] GI washout (Figure 4A) while the recovery of GI was accomplished more than 7 min after α-conotoxin GI washout (Figure 4B). [Y11A] GI at the concentration of 10 μM completely inhibited mouse α1β1δε nAChR and the inhibitory ACh-evoked current of [Y11A] GI was fully recovered within 2 min after α-conotoxin [Y11A] GI washout (Figure 4D). However, we noticed that 10 μM GI exhibited higher affinity on heteromeric α1β1δε nAChR, and the inhibitory ACh-evoked current of GI was only completely reversible over 9 min after α-conotoxin GI washout (Figure 4C). Table 1 summarizes the recovery time after blockade by α-conotoxin GI and its analogues.
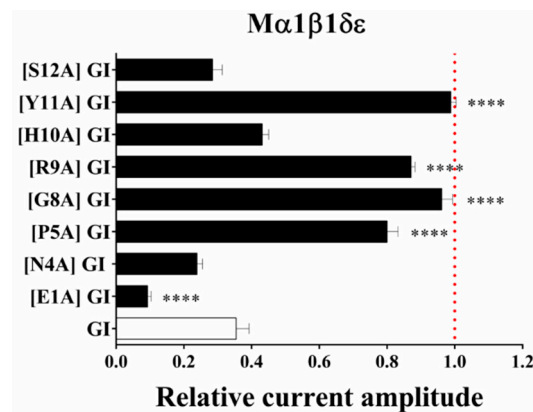
Figure 3. The effect on mouse α1β1δε expressed in *Xenopus laevis* oocytes by GI and alanine-substituted analogues. A bar graph of inhibition of mouse α1β1δε by GI and alanine variants. One-way analysis of variance scatter illustrating the loss or increase in the activity of alanine variants (10 nM) compared to wild peptide using Dunnett's multiple comparisons test. **** indicates *p* < 0.0001. All data represent mean ± S.E.M, *n* = 4–6.
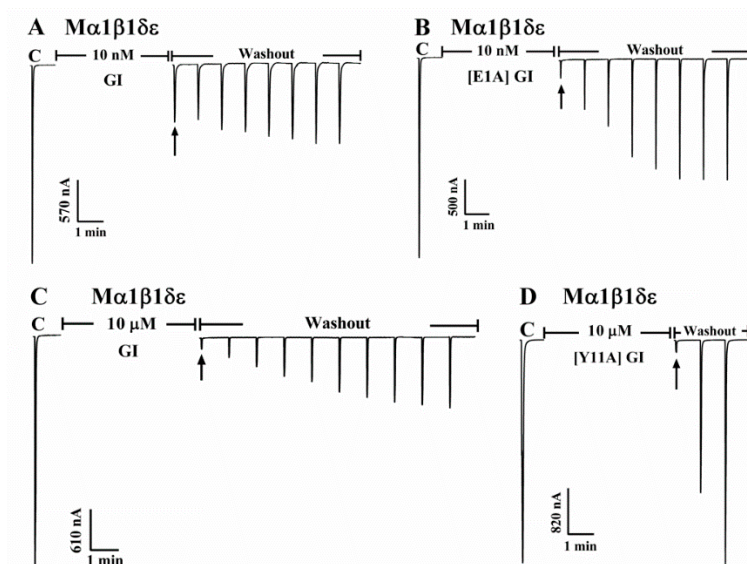

Figure 4. Blockade of mouse α1β1δε nAChR by GI, [E1A] GI and [Y11A] GI. Representative current traces showing the inhibition of mouse α1β1δε ACh-evoked currents by GI and [E1A] GI at the concentration of 10 nM (**A**, **B**), GI and [Y11A] GI at the concentration of 10 μM (**C**, **D**). *Xenopus laevis* oocytes expressing a given mouse α1β1δε nAChR were at a holding potential of −70 mV and were subjected to a 1 s pulse of ACh every minute as previously described [30]. After control responses to ACh, the oocyte was exposed to toxins for 5 min (arrow). The toxin was then washed out and the response to ACh was again measured. "C" indicates control responses to ACh.

Table 1. Recovery time after blockade by α-Conotoxin GI and its analogues at the mouse α1β1δε nAChR.

Peptides (10 nM)	T_{50} [a] (min)	Peptides (10 µM)	T_{95} [b] (min)
GI	>7	GI	>9
[E1A] GI	4	[Y11A] GI	2

[a] Time to 50% current amplitude recovery after toxin washout; GI and [E1A] GI were tested at a concentration of 10 nM. [b] Time to 95% current amplitude recovery after toxin washout; GI and [E1A] GI were tested at a concentration of 10 µM.

The concentration–response relationship of GI and its analogues were subsequently assessed on mouse α1β1δε nAChR. Figure 5B and Table 2 summarizes that the four analogues [P5A] GI, [G8A] GI, [R9A] GI and [Y11A] GI reduced the activity significantly and the concentration–response curves of them shifted rightward relative to the native GI. The potencies of [P5A] GI and [R9A] GI were 9.3-fold and 8.5-fold lower than GI. [P5A] GI and [R9A] GI inhibited α1β1δε nAChR with IC_{50} of 54.72 and 49.79 nM respectively (Figure 5B and Table 2). Furthermore, the substitution of Gly^8 and Tyr^{11} with Ala resulted in potencies more than 20-fold lower than GI. [G8A] GI and [Y11A] GI blocked muscle nAChR with IC_{50} of 170.60 and 381.20 nM respectively (Figure 5B and Table 2). Strikingly, when we substituted Glu^1 with Ala, the potency of [E1A] substantially increased with an IC_{50} of 1.83 nM (5.85 nM in GI) (Figure 5A and Table 2). The other three mutations, [N4A] GI, [H10A] GI and [S12A] GI preserved similar activity, when compared to wildtype GI (Table 2). Above all, our results demonstrated that a single amino acid substitution in GI had a significant impact on its activity.
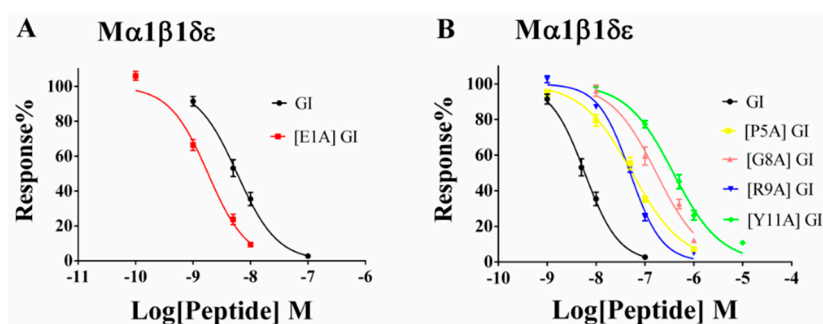
Figure 5. The concentration–response curves of mouse α1β1δε nAChR subtype for GI and alanine-substituted analogues. (**A**) The concentration–response curves for GI and [E1A] GI. peptide [E1A] GI shifted the curves to the left, relative to the parent peptide GI. (**B**) The concentration–response curves for GI, [P5A] GI, [G8A] GI, [R9A] GI and [Y11A] GI. [P5A] GI, [G8A] GI, [R9A] GI and [Y11A] GI were towards the right compared to the native GI. All data represent mean ± S.E.M, *n* = 7–10.

Table 2. IC_{50} and Hill slope values for inhibiting mouse α1β1δε subtype by α-conotoxin GI and its analogues.

| Name	IC_{50} (nM) * α1β1δε	nH	IC_{50} Ratio Relative to GI
GI	5.86 (5.01–6.86)	1.24 (0.93–1.55)	1.0
[E1A] GI	1.83 (1.55–2.15)	1.28 (1.06–1.51)	0.3
[N4A] GI	4.66 (4.19–5.18)	1.49 (1.23–1.76)	0.8
[P5A] GI	54.72(46.85–63.91)	0.84 (0.71–0.97)	9.3
[G8A] GI	170.60(134.60–216.30)	0.94 (0.74–1.13)	29.1
[R9A] GI	49.79 (45.22–54.81)	1.34 (1.13–1.54)	8.5
[H10A] GI	7.62 (6.78–8.57)	1.04 (0.88–1.20)	1.3
[Y11A] GI	381.20(323.40–449.40)	0.90 (0.76–1.05)	65.1
[S12A] GI	5.39 (4.72–6.15)	1.28 (1.01–1.55)	0.9

IC_{50} and nH indicates half inhibitory concentration and Hill Slope respectively. * indicates numbers in parentheses are 95% confidence intervals.

2.3. Potency of α-Conotoxin GI and Its Analogues at the Rat Neuronal nAChRs

Next, GI and above critical analogues were tested on other neuronal nAChR subtypes with high concentrations. Glu[1], Pro[5], Gly[8], Arg[9] and Tyr[11] harboring a substitution to Ala exhibited no activity on α3β2, α3β4, α4β4 and α7 subtypes even up to 10 μM (Figure 6). Interestingly, the inhibition of GI was 50% at the concentration of 10 μM and GI blocked ACh-evoked current of rα9α10 nAChR with an IC_{50} of 9.35 μM (Figure 7A and Table 3). Moreover, the potencies of [P5A] GI and [G8A] GI increased 2.1-fold and 2.2-fold compared to GI with the IC_{50} of 4.14 and 4.21 μM respectively (Figure 7 and Table 3). In contrast, replacing Glu[1] with Ala led to lower inhibitory activity on rα9α10 nAChR.
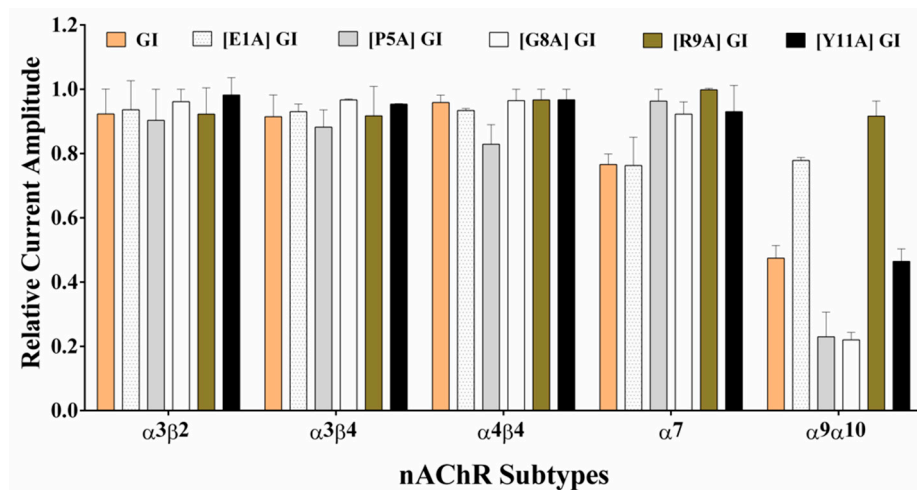
Figure 6. The effect of GI and alanine analogues on different nAChR subtypes expressed in *Xenopus laevis* oocytes. These mutations were determined at the concentration of 10 μM. A bar graph of the inhibition of nAChR subtypes by GI and its analogues. All data represent mean ± S.E.M, *n* = 4–6.
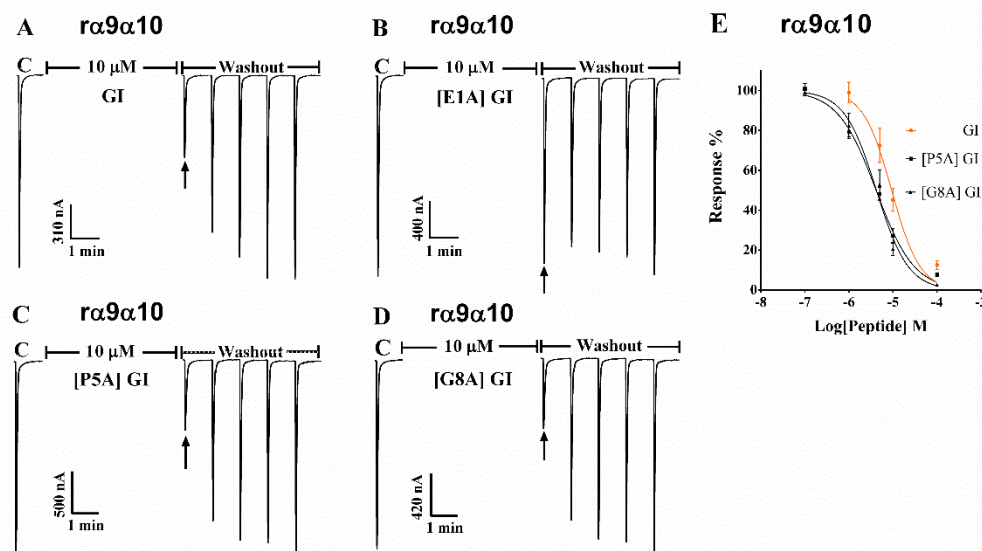
Figure 7. α-conotoxin GI and its analogues were tested on neuronal rat α9α10 nAChR subtype expressed in *Xenopus laevis* oocytes. The representative current traces showing the inhibition of rat α9α10 ACh-evoked currents by GI (**A**), [E1A] GI (**B**), [P5A] GI (**C**) and [G8A] GI (**D**) respectively. Oocytes were clamped at −70 mV holding potential, and membrane currents were evoked with 10 μM ACh. The inhibition of GI, [E1A] GI and [P5A] GI for rat α9α10 nAChR was 48.4%, 10.5%, 72.3% and 69.8% at the concentration of 10 μM respectively. (**E**) Concentration–response curves for GI, [P5A] GI and [G8A] GI. All data in (E) represent mean ± S.E.M, *n* = 5–8.

Table 3. IC_{50} and Hill slope values for inhibiting neuronal rat $\alpha 9 \alpha 10$ nAChR subtype by α-conotoxin GI and three mutants.

Name	IC_{50} (μM) * r$\alpha 9 \alpha 10$	nH	IC_{50} Ratio Relative to GI
GI	9.35 (7.02–12.5)	1.35 (0.57–2.15)	1
[E1A] GI	>10	-	-
[P5A] GI	4.14 (3.42–5.03)	1.01 (0.79–1.22)	0.4
[G8A] GI	4.21 (3.21–5.51)	1.20 (0.83–1.59)	0.5

IC_{50} and nH indicates half inhibitory concentration and Hill slope respectively. * indicates numbers in parentheses are 95% confidence intervals.

2.4. Homology Modeling and Molecular Dynamic Simulation

Molecular models of the interaction between the $\alpha 1(+)\delta(-)$ binding site and GI were established. The model was refined using molecular dynamics simulations; this was used to illuminate the SAR (Figure 8). According to the model, Glu^1 is surrounded by two cysteines (Cys^{176} and Cys^{177} in $\alpha 1$ subunit) forming disulfide (Figure 8A). Meanwhile, only one amino acid, Glu^{147} in the δ subunit was found to act with Glu^1, which would produce electrostatic repulsion. When Glu^1 was substituted by Ala, the repulsive force between them decreased, contributing to a three-fold increased blockade of $\alpha 1 \beta 1 \delta \varepsilon$ nAChR. Among all analogues, [Y11A] GI had the highest decrease at the potency on $\alpha 1 \beta 1 \delta \varepsilon$ nAChR. Through 40 ns dynamic stimulation, Tyr^{11} is impacted by more amino acids in the δ subunit, including Leu^{93}, Tyr^{95} and Leu^{103} (Figure 8B) forming a relatively hydrophobic environment. Replacing polar residue Tyr^{11} with a hydrophobic Ala significantly perturbed the affinity potency of GI to the δ subunit, explaining the activity loss of [Y11A] GI to $\alpha 1 \beta 1 \delta \varepsilon$ nAChR.
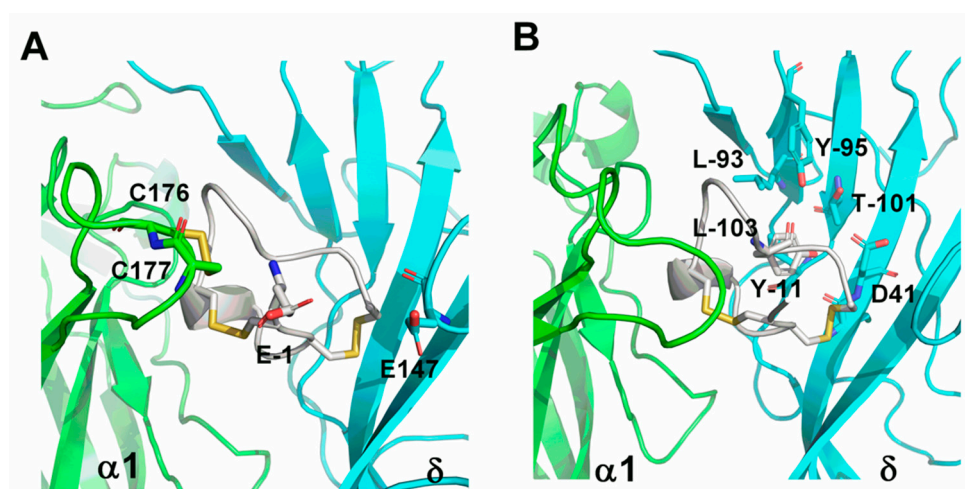
Figure 8. MD stimulations indicate the binding modes of GI to the interface of $\alpha \delta$ subunit respectively. (**A**) Amino acids around 5 Å radius of the Glu-1 of GI are labeled. (**B**) Amino acids around 4 Å radius of the Tyr-11 of GI are labeled. The $\alpha 1(+)$ subunit is shown in *green*, $\delta(-)$ subunit in *cyan* and the peptides GI in *white*.

3. Discussions

Until now, several conotoxins have been reported as muscle-type nAChRs inhibiters. The selected conotoxins from different *conus* species that targeted muscle-type nAChRs are summarized in Table 4. So far, five different families targeting the muscle-type nAChRs have been identified, including α-conotoxins, αB-conotoxins, αD-conotoxins, αO-conotoxins and αS-conotoxins, among which α-3/5 conotoxins become dominant with their high affinity and selectivity. Some conotoxins of other families also inhibited muscle nAChRs but with less selectivity. For example, αB-VxXXIVA cloned from *Conus vexillum* inhibited mouse $\alpha 1 \beta 1 \delta \varepsilon$ nAChR and rat $\alpha 9 \alpha 10$ nAChR with the IC_{50} of 6.6 μM and

1.2 µM, respectively [31,32]. Another conotoxin cloned from *Conus generalis*, named αO-GeXVIA, blocked various nAChR subtypes with nanomolar potency, including rat α9α10 nAChR and mouse α1β1δε nAChR [33]. Moreover, two other conotoxins also cloned from *Conus generalis,* named αD-GeXXA and αO-GeXXVIIA, blocked muscle-type nAChR and neuronal nAChRs [34,35].

The fetal muscle-type nAChRs contain two ligand binding sites located at the extracellular domain, α/γ or α/δ interface. The specific binding sites of these conotoxins have aroused attention, and several conotoxins were used to investigate the binding affinity on the α/γ or α/δ interface [20,36]. Firstly, three α-conotoxins, GI, MI and SIA conferred 10,000-fold greater affinity at the α/δ *versus* α/γ interface of muscle nAChR on BC3H-1 cells [20,37,38]. On the contrary, they displayed a higher affinity at the α/γ interface for *Torpedo* nAChR [39–41]. Hann et al. revealed that GI and MI exhibited similar physiological potencies on mouse nAChR while α-conotoxin SI was much less effective than them [21]. In addition, SI failed to discriminate between the α/γ and α/δ interface on mouse and *Torpedo* nAChR compared with GI or MI [21]. Previous investigation revealed that α-AC1.1b(CIA) from *Conus achatinus* strongly preferred the α/δ interface instead of the α/γ binding site on the mouse muscle nicotinic acetylcholine receptor [42]. Recently, Giribaldi et al. revealed that CIA also blocked the neuronal rat α3β2 nAChR with micromolar potency [43]. As we know, α-4/7-conotoxin was generally regarded as targeting various neuronal nAChRs, however, one α-4/7-conotoxin EI isolated from *Conus ermineus* was identified as selectively targeting the α/δ interface of the *Torpedo* muscle-type nAChRs [44], another α-4/7-conotoxin Lo1a has been characterized to differentiate between muscle-type nAChRs and neuronal-type nAChRs, and this conotoxin had a higher affinity at the α/ε interface [45]. Interestingly, αA-conotoxin OIVB with six cysteines isolated from *Conus obscurus* venoms from Indo-Pacific, exhibited 1800-fold lower affinity for adult muscle nAChRs, and this toxin preferentially bound to the α/γ interface [46]. Whereas ψ-conotoxin PrIIIE, with CysI–CysIV, CysII–CysV, and CysIII–CysVI disulfide configuration displays higher potency against the adult subtype than the fetal subtype nAChR [47,48].

The structure of GI was revealed by NMR spectroscopy and X-ray crystallography [19,24,49]. A right-handed helical turn containing an Asn[4]-Cys[7] β-turn in the Gly[8] to Tyr[11] region is a typical structural feature of GI [24]. Gray et al. assumed that the shape of peptide GI was a triangular slab with Glu[1], Pro[5] and Arg[9] situated at the corner [24]. As we know, the proline of loop1 in many α-conotoxins is conservative, and this amino acid plays a crucial role in 3_{10}-helix turn forming of conotoxins. Furthermore, Dutertre et al. demonstrated that 3_{10}-helix turn might play a crucial role in defining both the ligand conformation and receptor-binding activity [50]. Olivera, B. M el al. found that substituting Pro with Ala in α-conotoxin MI dramatically reduced the toxin's potency at the α/δ site [51]. Similarly, the Pro[5] mutation in GI might alter β-turn secondary structures, significantly reducing the activity of α1β1δε nAChR. Moreover, when we replaced Gly[8], Arg[9] and Tyr[11] with Ala, three analogues, [G8A] GI, [R9A] GI and [Y11A] GI, suffered respectively 29.1-fold, 8.5-fold and 65.1-fold loss of their potencies on α1β1δε nAChR compared to GI, suggesting that the substitution of Gly[8], Arg[9] and Tyr[11] with Ala probably had a significant impact on the right-handed helical turn. Meanwhile, Tyr[11] in α-conotoxin GI was located at a general hydrophobic pocket by molecular modeling, and we also noticed that it interacts with hydrophobic amino acids, including Leu[93], Tyr[95] and Leu[103] in the δ subunit (Figure 8B), which is consistent with previous studies that showed α-conotoxin MI interacted strongly with the δ subunit [40,41]. Janes, R. W et al. also suggested that a hydrophobic phenylalanine in this position contributed to anchoring to the receptor [52]. In contrast to the loss of inhibitory activity at most alanine substitutions, Glu[1] replaced by Ala in α-conotoxin GI substantially improved the functional activity at α1β1δε nAChR.

In addition, we observed a different current recovery time after the blockade by α-conotoxin GI, [E1A] GI and [Y11A] GI at the mouse α1β1δε nAChR, suggesting that single amino acid mutation possibly changed the interaction between ligands and receptors. Further research is needed in order to elucidate the molecular mechanism underlying their interaction. Various neuronal nAChRs, including α3β2, α3β4, α4β4, α7, and α9α10 were also screened. The electrophysiology assay indicated that

alanine-substituted analogues failed to inhibit these receptors, except for α9α10. GI, [P5A] GI and [G8A]GI retained their activity at α9α10 at the micromole level. In contrast, [E1A] GI had little influence on α9α10 nAChR at a high concentration, and the selectivity of [E1A] GI at muscle α1β1δε *versus* neuronal α9α10 nAChR was improved compared to wildtype GI.

Table 4. The sequences of conotoxins from different species of cone snails blocked muscle-type nAChRs.

Conotoxin	Resource	Sequence	Target	Reference
α-GI	*C. geographus*	ECCNPACGRHYSC*	muscle	[17,18]
α-MI	*C. magus*	GRCCHPACGKNYSC*	muscle	[51]
α-SI	*C. striatus*	ICCNPACGPKYSC*	muscle	[52]
α-SIA	*C. striatus*	YCCHPACGKNFDC*	muscle	[20]
α-AC1.1b/CIA	*C. achatinus*	NGRCCHPACGKHFSC*	muscle, α3β2	[42,43]
α-EI	*C. ermineus*	RDOCCYHPTCNMSNPQIC*	muscle, α3β4, α3β2, α4β2	[44]
α-Lo1a	*C. longurionis*	EGCCSNPACRTNHPEVCD	α7, α3β4, muscle	[45]
αA-OIVB	*C. obscurus*	CCGVONAACHOCVCKNTC*	muscle	[46]
αB-VxXXIVA	*C. vexillum*	VRCLEKSGAQPNKLFRPPCCQKG PSFARHSRCVYYTQSRE*	α9α10, muscle	[31,32]
αD-GeXXA	*C. generalis*	DVHRPCQSVRPGRVWGKCCLT RLCSTMCCARADCTCVYHTW RGHGCSCVM*	α9α10, α7, α3β4, α3β2, muscle	[34]
αO-GeXVIA	*C. generalis*	TCRSSGRYCRSPYDRRRRYCRRITD ACV*	α9α10, α7, α3β4, α3β2, muscle	[33]
αO-GeXXVIIA	*C. generalis*	ALMSTGTNYRLLKTCRGSGRYC RSPYDCRRRYCRRISDACV*	α9α10, muscle	[35]
Ψ-PrIIIE	*C. parius*	AARCCTYHGSCLKEK CRRKYCC*	muscle	[47,48]

For all conotoxins, an asterisk denotes a carboxyl-terminal carboxamide; O and γ indicates Hydroxyproline and γ-carboxyglutamate (Gla).

4. Materials and Methods

4.1. Peptide Synthesis and Oxidative Folding of α-Conotoxin GI and Its Analogues

All the α-conotoxin GI and its analogues' linear peptides were successfully synthesized using Fmoc chemistry and standard side protection, except for four cysteines [30]. The cysteine residues were orthogonally protected using the acid liable S-trityl groups and the acid-stable S-acetomedomethyl groups. After cleavage of the assembled peptide chain from the resin, the first disulfide bond (the S-trityl groups on CysI and CysIII) in each peptide was formed by incubating the peptides in 5 mM ferricyanide (pH 7.5, 0.2 mg/mL) 45 min at 25 °C. The second disulfide bond (S-acetomedomethyl groups on CysII and CysIV) was formed by incubating peptides in 0.4 mM I_2 (0.4 mg/mL) 1% TFA under nitrogen protection conditions for 10 min. Then the reaction was quenched by adding 1 M ascorbic acid until the mixture became colorless. The peptide was purified by preparative RP-HPLC. Analytical RP-HPLC and electrospray-mass spectroscopy (ESI-MS) confirmed the purity and molecular mass of oxidized peptides.

4.2. Peptide Quantification

The concentration of purified α-conotoxin GI and its analogues was quantified using an absorbance measurement with a spectrophotometer at a wavelength of 280 nm, calculated with the Lambert–Beer equation, a = εcl. Where A is the absorbance, ε is the extinction coefficient, l is the cuvette path length, c indicates the concentration, and ε is determined with the peptide properties calculator.

4.3. cRNA Preparation and Injection into Xenopus laevis Oocytes

Capped RNA (cRNA) for the various subunits were prepared using the mMESSAGE mMACHINE in vitro transcription Kit (Ambion, Austin, TX, USA) following linearization of the plasmid. The cRNA was purified using MEGA clearTm Transcription Clean-up Kit (Ambion, Austin, TX, USA).

The concentration of each cRNA was confirmed by Smart Spec™ plus Spectrophotometer (Bio-Rad, Hercules, CA, USA), with the absorbance monitored at 260 nm. Oocytes were extracted from mature female *Xenopus laevis* as described previously [30]. cRNAs of mouse α1, β1, δ, ε subunits were mixed at 2:1:1:1 ratio with the final concentration of approximately 50 ng/μL for each subunit cRNA. 50.6 nL of this mixture was injected into each *Xenopus lavies* oocyte using a Drummond microdispenser (Drummond Scientific, Broomall, PA, USA), and then were incubated at 17 °C in ND96 buffer (96.0 mM NaCl, 2.0 mM KCl, 1.8 mM CaCl₂, 1.0 mM MgCl₂, 5 mM HEPES, pH 7.1–7.5) supplemented with 10 μg/mL of penicillin, 10 μg/mL of streptomycin and 100 μg/mL of gentamicin before recording. Oocytes were injected within 1 day of harvesting and recordings were carried out 2–7 days after microinjection.

4.4. Two-Electrode Voltage Clamp Electrophysiological Recordings of nAChRs Expressed in Xenopus laevis Oocytes

Two-electrode voltage-clamp recordings from oocytes were carried out at room temperature using an Axonclamp 900A amplifier (molecular devices crop., Sunnyvale, CA, USA). The voltage-recording and current-injecting electrodes were pulled with borosilicate glass and had a resistance of 5–50 megaohms when supplemented with 3 M KCl. The concentration of ACh was 10 μM trials with α1β1δε and α9α10 subtypes, 200 μM trials with α7, and 100 μM for all other subtypes. Oocytes were exposed to a 50 μL cylindrical oocyte recording chamber fabricated from Sylgard, and it was gravity-perfused with ND96 buffer at a rate of ~2 mL/min. All toxin solutions also contained 0.1 mg/mL bovine serum albumin to reduce nonspecific adsorption of the peptide. During recording, the oocytes were clamped at a holding potential of −70 mV. Oocytes were gravity-perfused with standard ND96 solution and supplied once per minute with one second ACh pulse. As a stable baseline was achieved, either ND96 alone or ND96 containing varying concentrations of GI and its analogues were perfusion-applied in a static bath for 5 min before the agonist ACh was added. The electrophysiology data were recorded and analyzed using Clampfit 10.2 software (Molecular Devices Corp., Sunnyvale, CA, USA).

4.5. Data Analysis

The effects of α-conotoxin GI and its analogues on ACh-evoked nAChR-mediated currents were defined as peak current amplitudes relative to the average peak current amplitudes of three control ACh applications, and this was used to normalize the amplitude of each test response to obtain a "% response" or "% block". The concentration–response curves were fit to the pooled data by Equation (1).

$$\% \text{ response} = 100/\{1 + ([\text{toxin}]/\text{IC}_{50})^{\text{nH}}\}. \tag{1}$$

where nH is the slope factor (Hill slope) and IC_{50} is the peptide concentration that gave 50% inhibition of the maximal response. All the electrophysiological data were statistically analyzed using GraphPad Prism 6, with significant differences between the control GI and the analogues determined by t-test.

4.6. Molecular Modeling, Docking, and Dynamic Simulation

We resolve to clarify the molecular mechanism of GI and its analogues acting with muscle-type nAChRs. To begin, we constructed homology models of α1 and δ subunit with the program Modeler 9v10. Nicotinic acetylcholine receptor (code: 2BG9) from *Torpedo* was adopted as the template [53], and the interface was formed using *Lymnaea stagnalis* acetylcholine-binding protein (Ls-AChBP; PDB code: 1I9B) as the template [54]. Then the models were optimized with energy minimized by 100 ps of a standard molecular dynamic process with Gromacs 5.1. The structures of GI and its analog [Y11A] GI were used to dock to the α1δ nAChR interface using the program FlexpepDock. All dynamic simulations were performed using Gromacs 5.1. Each dynamic simulation

was performed for 40 ns. The interatomic contact difference plot was calculated by determining the total number of toxin contacts with 4 Å of each receptor residue.

5. Conclusions

In summary, we identified SAR between GI and the mouse α1β1δε nAChRs using an alanine-scan strategy. To be specific, peptide [E1A] GI selectively inhibited mouse α1β1δε nAChRs with better potency than native GI. Furthermore, [E1A] GI reduced the potency of neuronal α9α10 nAChRs subtype and improved its selectivity on mouse muscle nAChRs. Compared to wildtype GI, four peptides i.e., [P5A] GI, [G8A] GI, [R9A] GI and [Y11A] GI displayed a dramatic loss of activity at the mouse α1β1δε nAChR. Meanwhile, molecular dynamic simulations demonstrate a relatively hydrophobic Tyr[11] of GI, a critical residue, binding with the δ subunit at the mouse α1β1δε nAChR. For neuronal nAChRs, only two variants, [P5A] GI and [G8A] GI, have a slight increase at the α9α10 nAChR *versus* GI. Taken together, our work expanded our knowledge on SAR between GI and the muscle-type nAChRs, providing sufficient data for the redesign of GI analogues with higher affinity and selectivity.

References

1. Hurst, R.; Rollema, H.; Bertrand, D. Nicotinic acetylcholine receptors: From basic science to therapeutics. *Pharmacol. Therapeut.* **2013**, *137*, 22–54. [CrossRef] [PubMed]

2. Lebbe, E.K.; Peigneur, S.; Wijesekara, I.; Tytgat, J. Conotoxins Targeting Nicitinic Acetylcholine Receptor: An Overview. *Mar. Drugs* **2014**, *12*, 2970–3004. [CrossRef] [PubMed]

3. Mir, R.; Karim, S.; Kamal, M.A.; Wilson, C.M.; Mirza, Z. Conotoxins: Structure, Therapeutic Potential and Pharmacological Applications. *Curr. Pharm. Des.* **2016**, *22*, 582–589. [CrossRef] [PubMed]

4. Kalamida, D.; Poulas, K.; Avramopoulou, V.; Fostieri, E.; Lagoumintzis, G.; Lazaridis, K.; Sideri, A.; Zouridakis, M.; Tzartos, S.J. Muscle and neuronal nicotinic acetylcholine receptors. Structure, function and pathogenicity. *FEBS J.* **2007**, *274*, 3799–3845. [CrossRef] [PubMed]

5. Rogers, R.S.; Nishimune, H. The role of laminins in the organization and function of neuromuscular junctions. *Matrix Biol.* **2017**, *57–58*, 86–105. [CrossRef] [PubMed]

6. Saxena, A.; Stevens, J.; Cetin, H.; Koneczny, I.; Webster, R.; Lazaridis, K. Characterization of an anti-fetal AChR monoclonal antibody isolated from a myasthenia gravis patient. *Sci. Rep.* **2017**, *7*, 14426. [CrossRef] [PubMed]

7. Mott, M.; Luna, V.M.; Park, J.Y.; Downes, G.B.; Epley, K.; Ono, F. Expressing acetylcholine receptors after innervation suppresses spontaneous vesicle release and causes muscle fatigue. *Sci. Rep.* **2017**, *7*, 1674. [CrossRef]

8. Ching, K.H.; Burbelo, P.D.; Kimball, R.M.; Clawson, L.L.; Corse, A.M.; Iadarola, M.J. Recombinant expression of the nAChR-α1 subunit for the detection of conformation-dependent epitopes in Myasthenia Gravis. *Neuromuscul. Disord.* **2011**, *21*, 204–213. [CrossRef]

9. Olivera, B.M.; Teichert, R.W. Diversity of the neurotoxic *Conus* peptides: A model for concerted pharmacological discovery. *Mol. Interv.* **2007**, *7*, 251–260. [CrossRef]

10. Luo, S.; Zhu, X.; Wu, Y.; Zhangsun, D. Conotoxins and Drug Discovery with Special Reference to Hainan Species. In *Toxins and Drug Discovery*; Springer: Heidelberg, Germany, 2017; pp. 149–187.

11. Azam, L.; McIntosh, J.M. α-Conotoxins as pharmacological probes of nicotinic acetylcholine receptors. *Acta Pharmacol. Sin.* **2009**, *30*, 771–783. [CrossRef]

12. Albuquerque, E.X.; Pereira, E.F.; Alkondon, M.; Rogers, S.W. Mammalian nicotinic acetylcholine receptors: From structure to function. *Physiol. Rev.* **2009**, *89*, 73–120. [CrossRef] [PubMed]

13. Robinson, S.D.; Norton, R.S. Conotoxin gene superfamilies. *Mar. Drugs* **2014**, *12*, 6058–6101. [CrossRef] [PubMed]

14. Dao, F.-Y.; Yang, H.; Su, Z.-D.; Yang, W.; Wu, Y.; Hui, D.; Chen, W.; Tang, H.; Lin, H. Recent Advances in Conotoxin Classification by Using Machine Learning Methods. *Molecules* **2017**, *22*, 1057. [CrossRef]

15. Muttenthaler, M.; Akondi, K.B.; Alewood, P.F. Structure-activity studies on α-Conotoxins. *Curr. Pharm. Des.* **2011**, *17*, 4226–4241. [CrossRef] [PubMed]

16. Akondi, K.B.; Muttenthaler, M.; Dutertre, S.; Kaas, Q.; Craik, D.J.; Lewis, R.J.; Alewood, P.F. Discovery, synthesis, and structure-activity relationships of Conotoxins. *Chem. Rev.* **2014**, *114*, 5815–5847. [CrossRef] [PubMed]

17. Gray, W.R.; Luque, A.; Olivera, B.M. Peptide Toxins from *Conus geographus* Venom. *J. Biol. Chem.* **1981**, *256*, 4734–4740. [PubMed]

18. Johnson, D.S.; Martinez, J.; Eigoyhen, A.B.; Heinemann, S.F.; McIntosh, J.M. α-Conotoxin ImI exhibits subtype-specific nicotinic acetylcholine receptor blockade: Preferential inhibition of homomeric alpha 7 and alpha 9 receptors. *Mol. Pharmacol.* **1995**, *48*, 194–199.

19. Pardi, A.; Galdes, A.; Florances, J.; Maniconte, D. Solution Structures of α-Conotoxin GI Determined by Two-Dimensional NMR Spectroscopy. *Biochemistry* **1989**, *28*, 5494–5501. [CrossRef]

20. Groebe, D.R.; Dumm, J.M.; Levitan, E.S.; Abramson, S.N. alapha-Conotoxins selectively inhibited one of the two acetylcholine binding sites of nicotinic receptors. *Mol. Pharmacol.* **1995**, *48*, 105–111.

21. Hann, R.M.; Pagán, O.R.; Eterović, V.A. The α-Conotoxins GI and MI Distinguish between the Nicotinic Acetylcholine Receptor Agonist Sites while SI Does not. *Biochemistry* **1994**, *33*, 14058–14063. [CrossRef]

22. Hann, R.M.; Pagán, O.R.; Gregory, L.M.; Jácome, T.; Eterović, V.A. The 9-arginine residue of alpha-Conotoxin GI is responsible for its selective high affinity for the alphagamma agonist site on the electric organ acetylcholine receptor. *Biochemistry* **1997**, *36*, 9051–9056. [CrossRef] [PubMed]

23. Groebe, D.R.; Gray, W.R.; Abramson, S.N. Determinants involved in the affinity of alpha-Conotoxins GI and SI for the muscle subtype of nicotinic acetylcholine receptors. *Biochemistry* **1997**, *36*, 6469–6474. [CrossRef] [PubMed]

24. Guddat, L.W.; Martin, J.A.; Shan, L.; Edmundson, A.B.; Gray, W.R. Three-Dimensional Structure of the α-Conotoxin GI at 1.2 Å Resolution. *Biochemisty* **1996**, *35*, 11329–11335. [CrossRef] [PubMed]

25. Gehrmann, J.; Alewood, P.F.; Craik, D.J. Structure Determination of the three Disulfide Bond Isomers of α-Conotoxin GI: A Model for the Role of Disulfide Bonds in structural stability. *J. Mol. Biol.* **1998**, *278*, 401–415. [CrossRef] [PubMed]

26. Morrison, K.L.; Weiss, G.A. Combinatorial alanine-scanning. *Curr. Opin. Chem. Biol.* **2001**, *5*, 302–307. [CrossRef]

27. Eustache, S.; Leprince, J.; Tuffery, P. Progress with peptide scanning to study structure-activity relationships: The implications for drug discovery. *Expert Opin. Drugs* **2016**, *11*, 771–784. [CrossRef]

28. Myers, R.A.; Cruz, L.J.; Rivier, J.E.; Olivera, B.M. *Conus* peptides as chemical probes for receptors and ion channels. *Chem. Rev.* **1993**, *93*, 1923–1936. [CrossRef]

29. Myers, R.A.; Zafaralla, G.C.; Gray, W.R.; Abbott, J.; Cruz, L.J.; Olivera, B.M. α-Conotoxins, small peptide probes of nicotinic acetylcholine receptors. *Biochemistry* **1991**, *30*, 9370–9377. [CrossRef]

30. Luo, S.; Zhangsun, D.; Zhu, X.; Wu, Y.; Hu, Y.; Christensen, S. Characterization of a novel α-Conotoxin TxID from *Conus textile* that potently blocks rat alpha3beta4 nicotinic acetylcholine receptors. *J. Med. Chem.* **2013**, *56*, 9655–9663. [CrossRef]

31. Loughnan, M.; Nicke, A.; Jones, A.; Schroeder, C.I.; Nevin, S.T.; Adams, D.J. Identification of a novel class of nicotinic receptor antagonists: Dimeric Conotoxins VxXIIA, VxXIIB, and VxXIIC from *Conus vexillum*. *J. Biol. Chem.* **2006**, *281*, 24745–24755. [CrossRef]

32. Luo, S.; Christensen, S.; Zhangsun, D.; Wu, Y.; Hu, Y.; Zhu, X. A Novel Inhibitor of alapha9alapha10 Nicotinic Acetylcholine Receptors from *Conus vexillum* Delineates a New Conotoxin Superfamily. *PLoS ONE* **2013**, *8*, e54648.

33. Luo, S.; Zhangsun, D.; Harvey, P.J.; Kaas, Q.; Wu, Y.; Zhu, X. Cloning, synthesis, and characterization of αO-conotoxin GeXIVA, a potent alapha9alapha10 nicotinic acetylcholine receptor antagonist. *Proc. Natl. Acad. Sci. USA* **2015**, *112*, E4026–E4035. [CrossRef] [PubMed]

34. Xu, S.; Zhang, T.; Kompella, S.N.; Yan, M.; Lu, A.; Wang, Y. Conotoxin alphaD-GeXXA utilizes a novel strategy to antagonize nicotinic acetylcholine receptors. *Sci. Rep.* **2015**, *5*, 14261. [CrossRef] [PubMed]

35. Jiang, S.; Tae, H.S.; Xu, S.; Shao, X.; Adams, D.J.; Wang, C. Identification of a Novel O-Conotoxin Reveals an Unusual and Potent Inhibitor of the Human alpha9alpha10 Nicotinic Acetylcholine Receptor. *Mar. Drugs* **2017**, *15*, 170. [CrossRef] [PubMed]

36. Blount, P.; Merlie, J.P. Molecular Basis of the Two Nonequivalent Ligand Binding Sites of the Muscle Nicotinic Acetylcholine Receptor. *Neuron* **1989**, *3*, 349–357. [CrossRef]

37. Kreienkamp, H.J.; Sine, S.M.; Maeda, R.K.; Taylor, P. Glycosylation sites selectively interfere with alpha-toxin binding to the nicotinic acetylcholine receptor. *J. Biol. Chem.* **1994**, *269*, 8108–8114. [PubMed]

38. Luo, S.; McIntosh, J.M. Iodo-alpha-Conotoxin MI selectively binds the alpha/delta subunit interface of muscle nicotinic acetylcholine receptors. *Biochemistry* **2004**, *43*, 6656–6662. [CrossRef] [PubMed]

39. Bren, N.; Sine, S.M. Hydrophobic Pairwise Interactions Stabilize α-Conotoxin MI in the Muscle Acetylcholine Receptor Binding Site. *J. Biol. Chem.* **2000**, *275*, 12692–12700. [CrossRef]

40. Sine, S.M.; Kreienkamp, N.B.; Maeda, R.; Taylort, P. Molecular Dissection of Subunit Interfaces in the Acetylcholine Receptor: Identification of Determinants of α-Conotoxin MI Selectivity. *Neuropharmacology* **1995**, *15*, 205–211. [CrossRef]

41. Sugiyama, N.; Marchot, P.; Kawanishi, C.; Osaka, H.; Molles, B.; Sine, S.M. Residues at the Subunit Interfaces of the Nicotinic Acetylcholine Receptor That Contribute to α-Conotoxin MI Binding. *Mol. Pharmacol.* **1998**, *53*, 787–794. [CrossRef]

42. Liu, L.; Chew, G.; Hawrot, E.; Chi, C.; Wang, C. Two Potent alapha-3/5 Conotoxins from Piscivorous *Conus achatinus*. *Acta Biol. Biophys. Sin.* **2007**, *39*, 438–444. [CrossRef]

43. Giribaldi, J.; Wilson, D.; Nicke, A.; Laconde, G.; Faucherre, A. Synthesis, Structure and Biological Activity of CIA and CIB, Two α-Conotoxins from the Predation-Evoked Venom of *Conus catus*. *Toxins* **2018**, *10*, 222. [CrossRef] [PubMed]

44. Park, K.H.; Suk, J.E.; Jacobsen, R.; Gray, W.R.; McIntosh, J.M.; Han, K.H. Solution conformation of alpha-Conotoxin EI, a neuromuscular toxin specific for the alpha1/delta subunit interface of *torpedo* nicotinic acetylcholine receptor. *J. Biol. Chem.* **2001**, *276*, 49028–49033. [CrossRef] [PubMed]

45. Lebbe, E.K.; Peigneur, S.; Maiti, M.; Devi, P.; Ravichandran, S.; Lescrinier, E.; Ulens, C.; Waelkens, E.; D'Souza, L.; Herdewijn, P.; et al. Structure-function elucidation of a new α-Conotoxin, Lo1a, from *Conus longurionis*. *J. Biol. Chem.* **2014**, *289*, 9573–9583. [CrossRef] [PubMed]

46. Teichert, R.W.; Rivier, J.; Torres, J.; Dykert, J.; Miller, C.; Olivera, B.M. A uniquely selective inhibitor of the mammalian fetal neuromuscular nicotinic acetylcholine receptor. *J. Neurosci.* **2005**, *25*, 732–736. [CrossRef] [PubMed]

47. Liuisma, A.O.; López-Vera, E.; Bulaj, G.; Watkins, M.; Olivera, B.M. Characterization of a novel ψ-Conotoxin from *Conus parius*. *Toxicon* **2008**, *51*, 174–180. [CrossRef] [PubMed]

48. Mitchell, S.S.; Shon, K.J.; Foster, M.P.; Davis, D.R.; Olivera, B.M.; Ireland, C.M. Three-Dimensional Solution Structure of Conotoxin ψ-PIIIE, an Acetylcholine Gated Ion Channel Antagonist. *Biochemistry* **1998**, *37*, 1215–1220. [CrossRef]

49. Maslennikov, I.V.; Sobol, A.G.; Gladky, K.V.; Lugovskoy, A.A.; Ostrovsky, A.G.; Tsetlin, V.I.; Ivanov, V.T.; Arseniev, A.S. Two distinct structures of α-Conotoxin GI in aqueous solution. *Eur. J. Biochem.* **1998**, *254*, 238–247. [CrossRef]

50. Dutertre, S.; Lewis, R.J. Toxin insights into nicotinic acetylcholine receptors. *Biochem. Pharmacol.* **2006**, *72*, 661–670. [CrossRef]

51. Jacobsen, R.B.; DelaCruz, R.G.; Grose, J.H.; McIntosh, J.M.; Yoshikami, D.; Olivera, B.M. Critical Residues Influence the Affinity and Selectivity of α-Conotoxin MI for Nicotinic Acetylcholine Receptors. *Biochemisty* **1999**, *38*, 13310–13315. [CrossRef]

52. Benie, A.J.; Whitford, D.; Hargittai, B.; Barany, G.; Janes, R.W. Solution structure of α-Conotoxin SI. *FEBS J.* **2000**, *476*, 287–295. [CrossRef]

53. Unwin, N. Refined structure of the nicotinic acetylcholine receptor at 4Å resolution. *J. Mol. Biol.* **2005**, *346*, 967–989. [CrossRef] [PubMed]

54. Brejc, K.; Van Dijk, W.J.; Klaassen, R.V.; Schuurmans, M.; Smit, A.B.; Sixma, T.K. Crystal structure of an ACh-binding protein reveals the ligand-binding domain of nicotinic receptors. *Nature* **2001**, *411*, 269–276. [CrossRef] [PubMed]